

AD-A163 367

WHISTLER-MODE RADIATION FROM THE SPACELAB 2 ELECTRON
BEAM(U) IOWA UNIV IOWA CITY DEPT OF PHYSICS AND
ASTRONOMY D A GURNETT ET AL 27 NOV 85

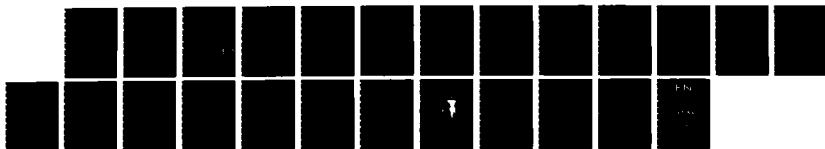
1/1

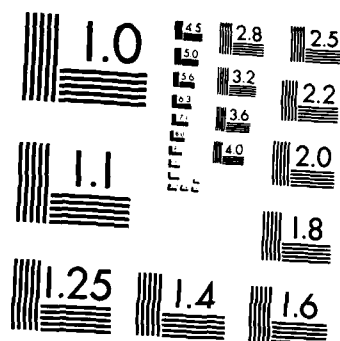
UNCLASSIFIED

U OF IOWA-85-19 N00014-85-K-0404

F/G 22/1

NL





MICROCOPY RESOLUTION TEST CHART
NATIONAL BUREAU OF STANDARDS-1963-A

12

AD-A163 367

WHISTLER-MODE RADIATION FROM THE
SPACELAB 2 ELECTRON BEAM

by

D. A. Gurnett¹, W. S. Kurth², J. T. Fainberg¹,
P. M. Banks², E. J. Bush² and W. J. Raitt³



UIC
C. J. Fainberg
J. T. Fainberg
J. T. Fainberg

U.S. GOVERNMENT PRINTING OFFICE
WASHINGTON, D.C. 20540
1985

Department of Physics, University of Iowa
Iowa City, Iowa 52242
U.S. GOVERNMENT PRINTING OFFICE

WHISTLER-MODE RADIATION FROM THE
SPACELAB 2 ELECTRON BEAM

by

D. A. Gurnett¹, W. S. Kurth¹, J. T. Steinberg¹,
P. M. Banks², R. I. Bush² and W. J. Raitt³

November 1985

DTIC
ELECTE
S JAN 28 1986 D
B

¹Department of Physics and Astronomy, University of Iowa, Iowa City,
Iowa 52242

²Department of Electrical Engineering, Stanford University, Stanford,
California 94305

³Center for Atmospheric and Space Science, Utah State University,
Logan, Utah 84322

DISTRIBUTION STATEMENT A

Approved for public release
Distribution Unlimited

UNCLASSIFIED

SECURITY CLASSIFICATION OF THIS PAGE (When Data Entered)

REPORT DOCUMENTATION PAGE		READ INSTRUCTIONS BEFORE COMPLETING FORM
1. REPORT NUMBER U. of Iowa 85-19	2. GOVT ACCESSION NO. AD-4163	3. RECIPIENT'S CATALOG NUMBER 367
4. TITLE (and Subtitle) Whistler-Mode Radiation from the Spacelab 2 Electron Beam		5. TYPE OF REPORT & PERIOD COVERED Progress November 1985
		6. PERFORMING ORG. REPORT NUMBER
7. AUTHOR(s) D. A. Gurnett, W. S. Kurth, J. T. Steinberg, P. M. Banks, R. I. Bush, and W. J. Raitt		8. CONTRACT OR GRANT NUMBER(s) N00014-85-K-0404
9. PERFORMING ORGANIZATION NAME AND ADDRESS Dept. of Physics and Astronomy The University of Iowa Iowa City, IA 52242		10. PROGRAM ELEMENT, PROJECT, TASK AREA & WORK UNIT NUMBERS
11. CONTROLLING OFFICE NAME AND ADDRESS Electronics Program Office Office of Naval Research Arlington, VA 22217		12. REPORT DATE 27 November 1985
		13. NUMBER OF PAGES 21
14. MONITORING AGENCY NAME & ADDRESS (if different from Controlling Office)		15. SECURITY CLASS. (of this report) Unclassified
		15a. DECLASSIFICATION/DOWNGRADING SCHEDULE
16. DISTRIBUTION STATEMENT (of this Report) Approved for public release; distribution is unlimited.		
17. DISTRIBUTION STATEMENT (of the abstract entered in Block 20, if different from Report)		
18. SUPPLEMENTARY NOTES		
19. KEY WORDS (Continue on reverse side if necessary and identify by block number) Whistler-mode radiation Shuttle PDP Spacelab 2		
20. ABSTRACT (Continue on reverse side if necessary and identify by block number) (See following page)		

ABSTRACT

During the Spacelab 2 mission the Plasma Diagnostics Package (PDP) performed a fly-around of the shuttle at distances of up to 300 meters while an electron beam was being ejected from the shuttle. This paper discusses a magnetic conjunction of the shuttle and the PDP while the electron gun was operating in a steady (DC) mode. During this conjunction the PDP detected a very clear funnel-shaped emission that is believed to be caused by whistler-mode emission from the beam. Ray path calculations show that the shape of the funnel can be accounted for by whistler-mode waves propagating near the resonance cone. Since the beam and waves are propagating in the same direction, the radiation must be produced by a Landau, $\omega/k_{\parallel} = v_b$, interaction with the beam. Other types of waves generated by the beam are also described.

Accession For	
NTIS	✓
DTL	
Uncl.	
Ja	
By	
Dist	
Avail	
Dist	
A-1	



I. INTRODUCTION

During the recent Spacelab 2 flight, which was launched on July 29, 1985, a spacecraft called the Plasma Diagnostics Package (PDP) was released from the shuttle to survey the plasma environment around the shuttle. Among the various investigations performed was a study of the effects produced by an electron beam ejected from the shuttle. This paper describes the plasma waves observed during a magnetic conjunction between the PDP and the shuttle while the electron gun was being operated. As will be shown, the plasma wave emissions observed are remarkably similar to emissions detected by spacecraft flying through auroral electron beams.

The PDP was designed and constructed at The University of Iowa and is a reflight of the spacecraft previously flown on the STS-3 flight [Shawhan et al., 1984]. The PDP included instrumentation from The University of Iowa, Goddard Space Flight Center, and Marshall Space Flight Center. For a description of the spacecraft and instruments, see Shawhan [1982]. The electron gun on the shuttle is part of the Vehicle Charging and Potential (VCAP) experiment which was provided by Stanford University and Utah State University. For a description of the VCAP instrumentation, see Raitt et al. [1982].

The Spacelab 2 mission was flown in a nearly circular low-inclination orbit with a nominal altitude of about 325 km and an inclination of 49.5° . The PDP was in free flight around the shuttle

from 0010 to 0620 UT on August 1, 1985. During this roughly 6-hour interval the shuttle performed two complete fly-arounds of the PDP. These fly-arounds included four magnetic conjunctions in which the shuttle was targeted to intersect the magnetic field line passing through the PDP. During the first two conjunctions the electron gun was off so that the PDP could monitor disturbances produced in the ionosphere by the shuttle. During the third conjunction, which is discussed here, the gun was operated in a steady (DC) mode to simulate a natural aurora, and during the fourth conjunction the gun was operated in a pulsed mode.

II. OBSERVATIONS

The trajectory of the shuttle relative to the PDP during the third conjunction is shown in Figure 1. The coordinate system used in this diagram is the so-called local-vertical, local-horizontal system. The z axis is directed toward the center of the earth, the x axis is in the orbital plane, and the y axis completes the usual right-handed coordinate system. Time is shown by the tick marks along the trajectory. A complete fly-around takes one orbit, or about 92 minutes. The magnetic conjunction of interest occurred at 0334:12 UT. The magnetic field at the time of the conjunction is shown in Figure 1 projected onto the x - z plane. The (x,y,z) coordinates of the shuttle at this time are $(-53, 89, -188)$ meters, and the separation distance is 216 meters. Calculations based on a model magnetic field indicate that the magnetic field line through the shuttle came within 10 meters of the PDP.

A spectrogram of the plasma wave electric field intensities during a 30-minute period around the magnetic conjunction is shown in Figure 2. These measurements are from the 3.89 meter double-sphere electric antenna on the PDP. The frequency range extends from 31 Hz to 17.8 MHz and the dynamic range extends from about 10^{-14} to 10^{-6} volts²m⁻²Hz⁻¹. The perpendicular distance, R_{\perp} , in meters, from the PDP to the magnetic field line through the shuttle is shown at the bottom

of the spectrogram. The electron gun was turned on in the steady (DC) mode with a beam energy of 1 keV and current of 50 mA at 0330:00 UT and stayed on until 0337:40 UT. During this period the shuttle was oriented such that the electron beam was ejected downward toward the PDP, as shown in Figure 1.

The intense nearly symmetric emission centered on about 0334:05 UT in Figure 2 is produced by the electron beam. At low frequencies the spectrum is characterized by a very intense broadband emission from about 0333:20 UT to 0334:20 UT. Another type of low frequency noise can be seen extending from about 0328 to 0339. This noise is produced by an interaction of the shuttle with the ionosphere and is not related to the electron beam. At higher frequencies a very well defined funnel-shaped feature can be seen extending up to about 1 MHz, spreading out at higher frequencies. The upper cutoff of the funnel-shaped emission is just below the electron cyclotron frequency, which is shown by the solid line labelled f_c in Figure 2. The onset and termination of the funnel at 0330:00 UT and 0337:40 UT correspond to the start and stop times of the electron gun operation. At even higher frequencies an intense narrowband emission can be seen at about 3.1 MHz, lasting for about 30 seconds, from 0333:45 to 0334:15 UT. From a preliminary comparison with the electron density [N. D'Angelo, personal communication], it is believed that this narrowband emission is at either the electron plasma frequency, f_p , or the upper hybrid resonance frequency, $f_{UHR} = (f_c^2 + f_p^2)^{1/2}$. For $f_p \approx 3.1$ MHz and $f_c \approx 1$ MHz, both of these frequencies are nearly the same, so it is difficult to be sure which is the relevant frequency.

Representative plots of the electric and magnetic field spectrums are shown in Figure 3. The spectrum at 0334:00 UT shows the intensities near the beam, and the spectrum at 0335:00 UT shows the intensities away from the beam. Near the beam both the electric and magnetic intensities are above the instrument noise level over the entire frequency range measured. The narrowband emission near the plasma frequency is clearly evident. The electric field strength of this emission is about 2.8 mVolts/m. Although this emission is most likely an electrostatic wave, the electrostatic/electromagnetic character cannot be clearly established because no magnetic field measurements are available in this frequency range. Near the beam, at 0334:00 UT it is difficult to distinguish the funnel-shaped emission above about 10 kHz from the intense low frequency noise below 10 kHz. Both types of emissions have a magnetic field component. The electric field strength of the low frequency noise, integrated from 31 Hz to 10 kHz, is about 150 mVolt/m, and the magnetic field strength integrated over the same frequency range, is about 0.17 nT. As a crude indication of the electrostatic/electromagnetic character of this noise one can compute the magnetic to electric field ratio, cB/E , and compare this ratio to the expected index of refraction for an electromagnetic wave. The cB/E ratio is shown in the bottom panel of Figure 3. The cB/E ratio of the low frequency noise varies from 3.0 to 30, less than would be expected for a purely electromagnetic mode of propagation. For reference the index of refraction, n , for parallel propagation is shown in Figure 3. The field strength of the funnel-shaped emission is best determined in

the region away from the beam, at 0335:00 UT, where it can be clearly distinguished from the low frequency noise. The broadband electric and magnetic field strengths, integrated over the emission bandwidth, are 7.5 mVolts/m and 0.1 nT. Again the cB/E ratio is less than would be expected for parallel propagation.

III. INTERPRETATION

The plasma wave emissions from the SL-2 electron beam bear a close similarity to waves observed in the earth's auroral zones. The most remarkable similarity is the funnel-shaped emissions. Very similar funnel-shaped emissions have been observed on a variety of polar orbiting spacecraft and have been called V-shape hiss, saucers and funnels [Gurnett, 1966; Smith, 1969; Mosier and Gurnett, 1969; Gurnett and Frank, 1972; James, 1976; Gurnett et al., 1983]. These emissions are a special case of a general class of emissions known as auroral hiss [Helliwell, 1965]. It is widely believed that this noise is whistler-mode radiation produced by electron beams associated with the aurora [Gurnett, 1966; Hartz, 1971; Hoffman and Laaspere, 1972; Gurnett and Frank, 1972].

The funnel-shaped spectral feature has a simple explanation based on the propagation of whistler-mode waves near the resonance cone. For wave normal angles near the resonance cone the ray propagates at an angle ψ_{Res} with respect to the magnetic field, as illustrated in Figure 4. The angle ψ_{Res} is given by

$$\tan^2 \psi_{\text{Res}} = - \frac{S}{P} = \frac{f^2}{f_c^2 - f^2} \quad , \quad (1)$$

where S and P are defined by Stix [1962]. The approximation is valid in the high density limit, where the wave frequency and electron cyclotron frequency are much less than the electron plasma frequency. Equation 1 shows that at low frequencies the ray path is almost exactly along the magnetic field. As the frequency increases the ray angle increases, approaching perpendicular as the wave frequency approaches the cyclotron frequency. Propagation ceases at frequencies above the cyclotron frequency. For a spatially localized line source, this frequency dependence produces a funnel-shaped frequency-time variation as the spacecraft crosses the source, as illustrated in Figure 4. The fact that the funnel is filled in indicates that the source is an extended (line) source. The sharply defined outer boundary indicates that the source starts at a well-defined point. The starting point is the electron gun in the case of the SL-2 electron beam, and the acceleration region in the case of the aurora.

To verify that the funnel-shaped emission observed by the PDP is caused by whistler-mode radiation near the resonance cone we have computed the limiting ray paths from the electron beam and compared the boundaries with the observed shape of the funnel. The results of these calculations are shown in Figure 5. The cross-hatched region shows the outline of the funnel, and the solid lines show the boundaries from the ray path computations. Since the distances involved are small compared to the spatial scale lengths in the ionosphere, the ray paths were assumed to be straight lines. The finite size of the beam was included, assuming a beam diameter of 5.2 meters. The actual equations

for S and P were used, including electrons but no ions. The electron cyclotron frequency and magnetic field direction were obtained from a multipole expansion of the earth's magnetic field. The computations are relatively insensitive to the electron plasma frequency. To provide a realistic value, $f_p = 3.1$ MHz was used. As can be seen from Figure 5, the ray path computations are in good agreement with the observations.

The whistler-mode interpretation of the funnel-shaped emission is also consistent with the observed magnetic to electric field ratio. For whistler-mode waves propagating near the resonance cone the electric field is stronger than for parallel propagation. This explains why the cB/E ratio is smaller than for parallel propagation. The observed ratios, $cB/E \sim 1$ to 10, are also consistent with the magnetic to electric field ratios measured for whistler-mode auroral hiss [Gurnett and Frank, 1972]. The existence of an easily detectable magnetic field also rules out the possibility that the noise could be an electrostatic electron acoustic mode, as has been suggested by Tokar and Gary [1984]. Also, there is no evidence of waves propagating in the opposite direction of the beam. Therefore, the radiation can be entirely attributed to the Landau resonance at $\omega/k_{\parallel} = v_b$.

Although the funnel-shaped emission is almost certainly whistler-mode radiation, the mode responsible for the more intense noise at lower frequencies has not been established. Although this noise appears to be a simple extension of the whistler-mode noise to lower frequencies there are several problems with attributing this noise to

the whistler mode. First, at low frequencies, below the lower hybrid frequency, which should be around 5.8 kHz, the whistler mode no longer has a resonance cone. Quasi-electrostatic propagation along the resonance cone is no longer possible. Second, at low frequencies the wavelength of the whistler mode becomes very large for all directions of propagation, much larger than the spatial thickness of the region of low frequency electrostatic noise, which is not more than a few tens of meters in diameter. Evidently this intense low frequency noise is caused by a local beam-generated instability. For a discussion of possible beam instabilities that could account for this noise, see Grandel [1982]. It is interesting to note that this noise has a spectrum very similar to the broadband electrostatic noise observed by Gurnett and Frank [1977] along the auroral field lines.

ACKNOWLEDGEMENTS

The research at the University of Iowa was supported by NASA through contract NAS8-32807, and grants NGL-16-001-043 and NGL-16-001-002, and by the Office of Naval Research through grant N00014-85-K-0404. The research at Stanford University was supported by contract NAS8-36011 and grant NAGW-235. The research at Utah State University was supported by subcontract PR3936 with Stanford University.

REFERENCES

- Grandel, B., Artificial Particle Beams in Space Plasma Studies, Plenum, N. York, 1982.
- Gurnett, D. A., A satellite study of VLF hiss, J. Geophys. Res., 71, 5599-5615, 1966.
- Gurnett, D. A., and L. A. Frank, VLF hiss and related plasma observations in the polar magnetosphere, J. Geophys. Res., 77, 172-190, 1972.
- Gurnett, D. A., and L. A. Frank, A region of intense plasma wave turbulence on auroral field lines, J. Geophys. Res., 82, 1031-1050, 1977.
- Gurnett, D. A., S. D. Shawhan and R. R. Shaw, Auroral hiss, z-mode radiation, and auroral kilometric radiation in the polar magnetosphere: DE 1 observations, J. Geophys. Res., 88, 329-340, 1983.
- Hartz, T. R., Particle precipitation patterns, The Radiating Atmosphere, 1970, ed. by B. McCormac, 222, Von Nostrand Reinhold, N. York, 1971.
- Helliwell, R. A., Whistlers and Related Ionospheric Phenomena, Stanford University Press, Stanford, 207, 1965.
- Hoffman, R. A., and T. Laaspere, Comparison of very-low-frequency auroral hiss with precipitating low-energy electrons by the use of simultaneous data from two OGO 4 experiments, J. Geophys. Res., 77, 640-650, 1972.

- James, H. G., VLF saucers, J. Geophys. Res., 81, 501-514, 1976.
- Mosier, S. R., and D. A. Gurnett, VLF measurements of the Poynting flux along the geomagnetic field with the Injun 5 satellite, J. Geophys. Res., 74, 5675-5687, 1969.
- Raitt, W. J., P. M. Banks, W. F. Denig, and H. R. Anderson, Transient effect in beam-plasma interactions in a space simulation chamber stimulated by a fast pulse electron gun, Artificial Particle Beams in Space Plasma Studies, ed. by B. Grandel, 405-418, Plenum, N. York, 1982.
- Shawhan, S. D., Description of the plasma diagnostics package (PDP) for the OSS-1 shuttle mission and JSC chamber test in conjunction with the fast pulse electron gun (FPEG), Artificial Particle Beams in Space Plasma Studies, ed. B. Grandel, 419-430, Plenum, N. York, 1982.
- Shawhan, S. D., G. B. Murphy, P. M. Banks, P. R. Williamson and W. J. Raitt, Wave emissions from dc and modulated electron beams on STS-3, Radio Science, 19, 471-486, 1984.
- Smith, R. L., VLF observations of auroral beams as sources of a class of emission, Nature, 224, 351-352, 1969.
- Stix, T. H., The Theory of Plasma Waves, McGraw-Hill, N. York, 10, 1962.
- Tokar, R. L., and S. P. Gary, Electrostatic hiss and the beam driven electron acoustic instability in the dayside polar cusp, Geophys. Res. Lett., 11, 1180-1183, 1984.

FIGURE CAPTIONS

- Fig. 1. The trajectory of the shuttle relative to the PDP during the third magnetic conjunction. The electron beam was ejected downward, toward the PDP.
- Fig. 2. A spectrogram of the plasma wave electric field intensities during the third magnetic conjunction.
- Fig. 3. Electric and magnetic spectrums, $E^2/\Delta f$ and $B^2/\Delta f$, and the magnetic to electric field ratio, cB/E , averaged over 30-sec. intervals near the magnetic conjunction, 0334:00, and shortly after the magnetic conjunction, 0335:00 UT.
- Fig. 4. A schematic illustration showing the ray paths of whistler-mode radiation from a point source for wave normal angles near the resonance cone. The ray path angle ψ increases with increasing frequency, thereby producing a funnel-shaped feature as the spacecraft crosses the source field line.
- Fig. 5. A comparison of the computed ray path boundaries with the observed shape of the funnel-shaped emission. The close agreement indicates that the radiation is produced by whistler mode waves propagating near the resonance cone.

C-685-790

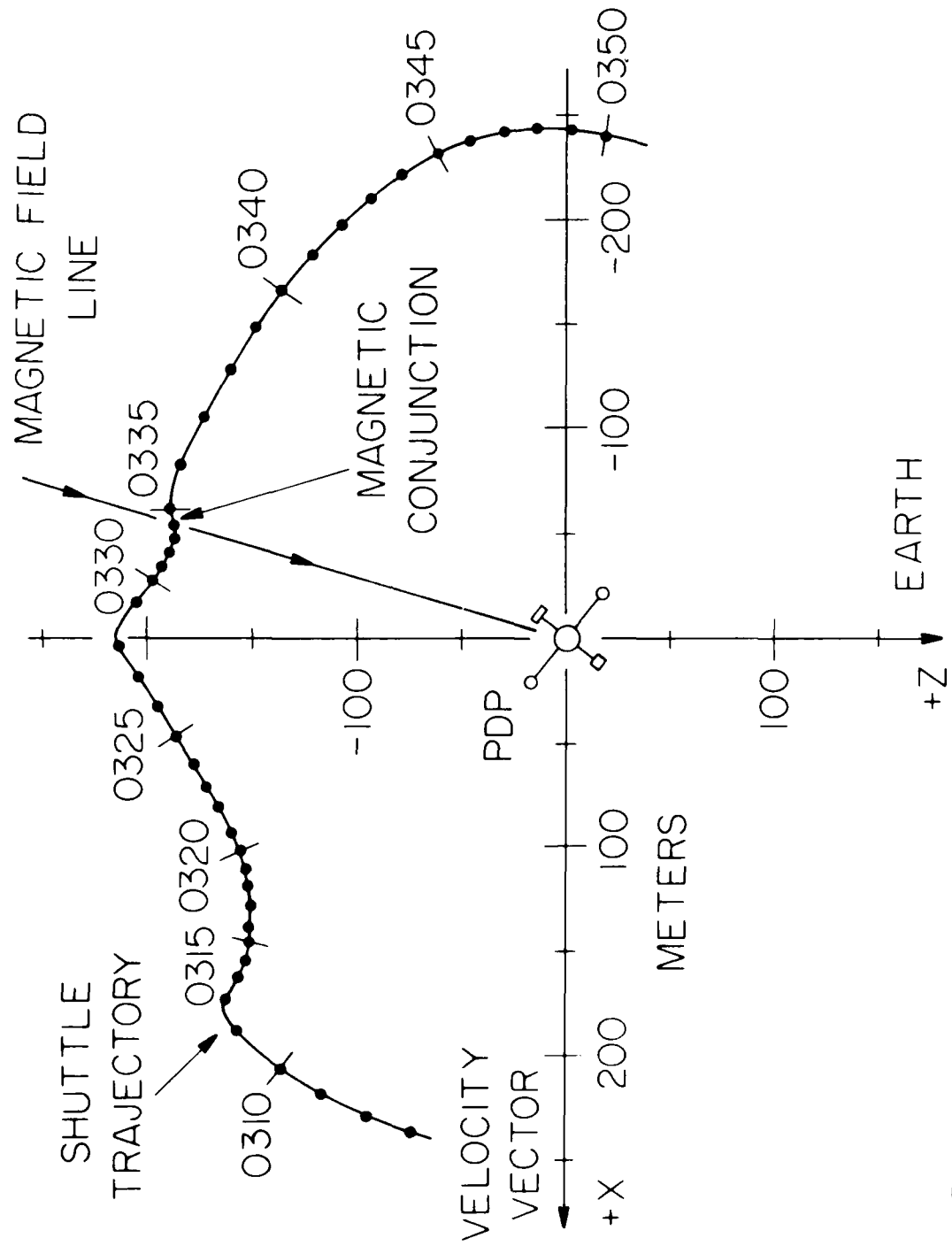


Figure 1

A-G85-807-1

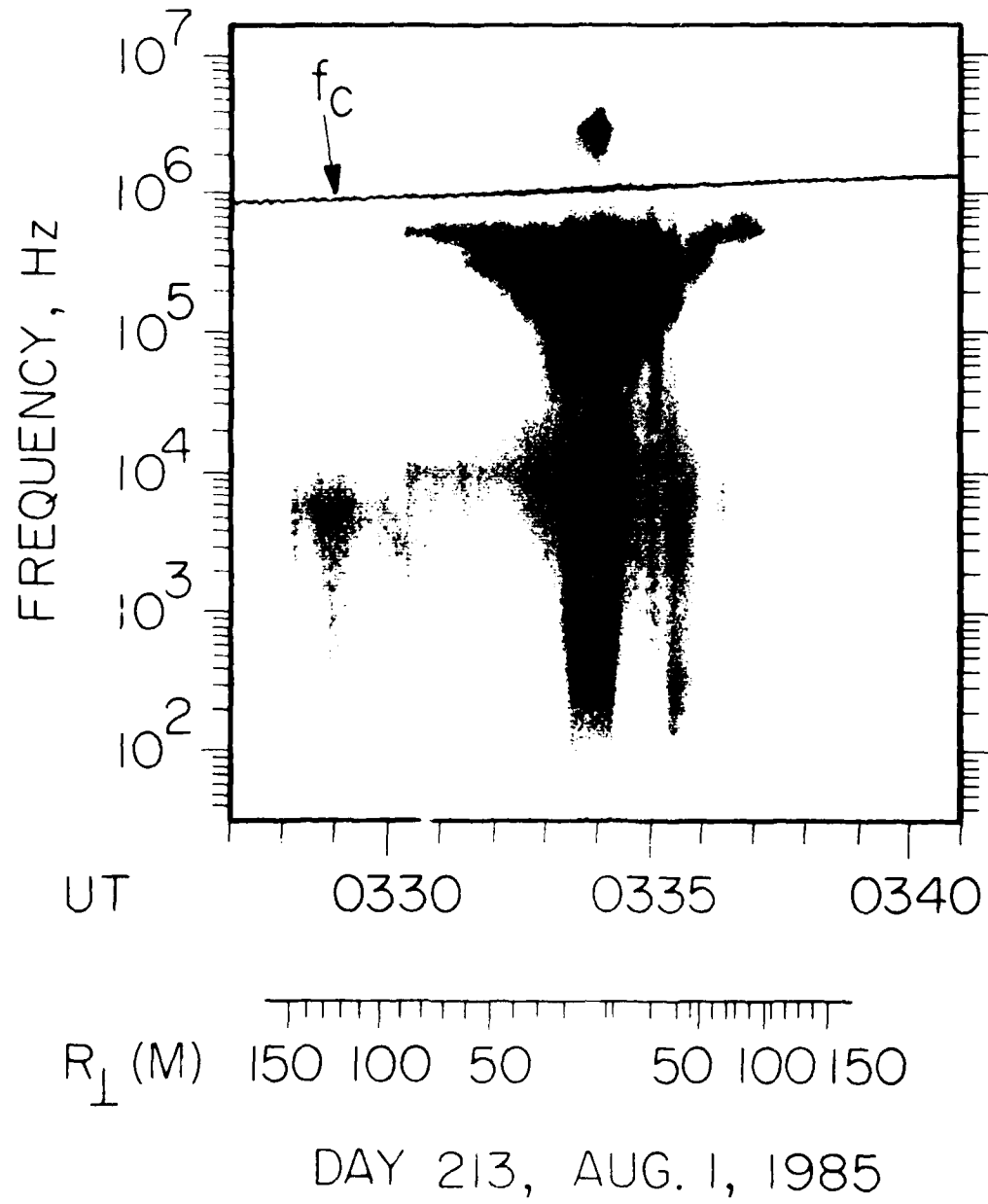


Figure 2

B-G85-793-1

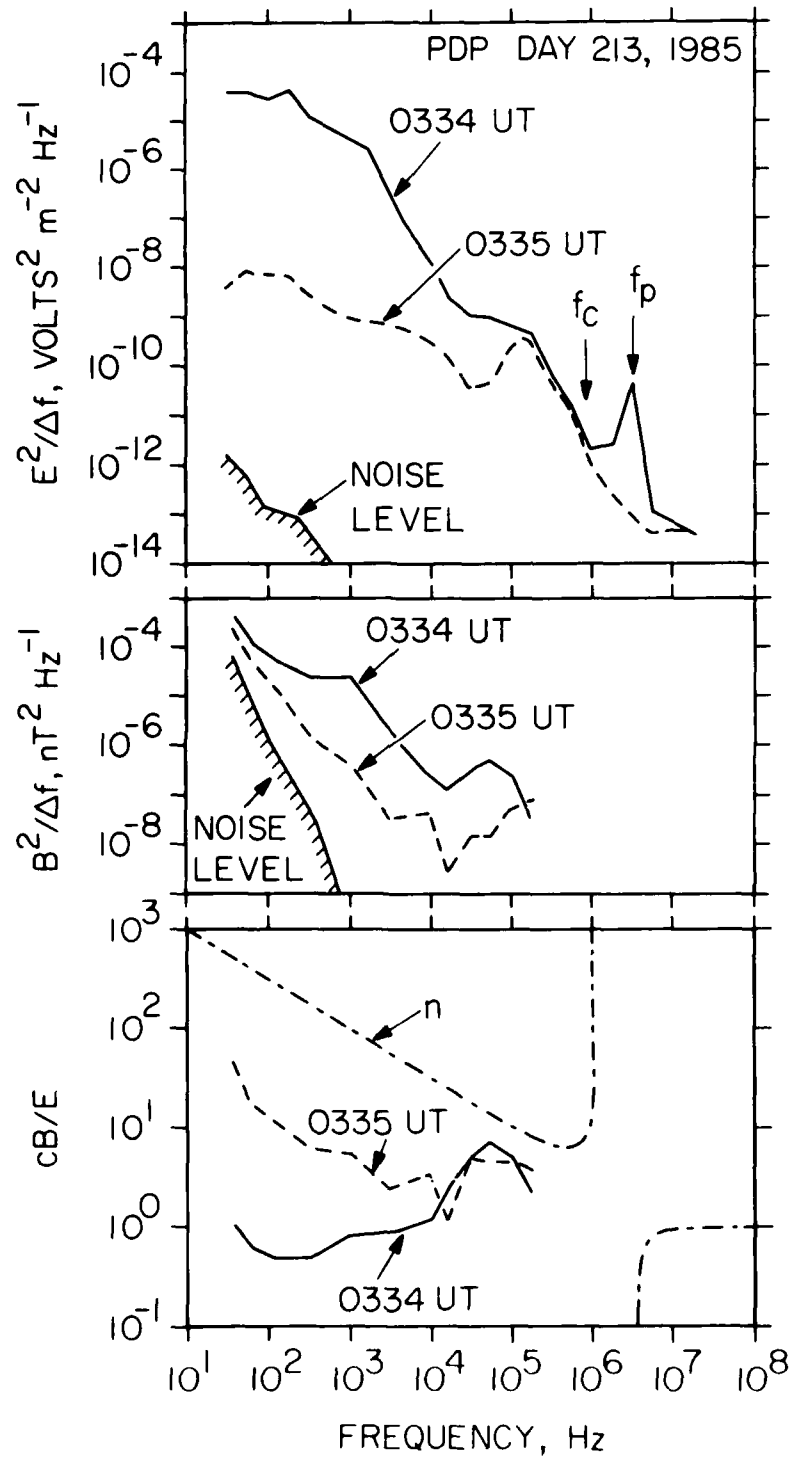


Figure 3

B-G85-792

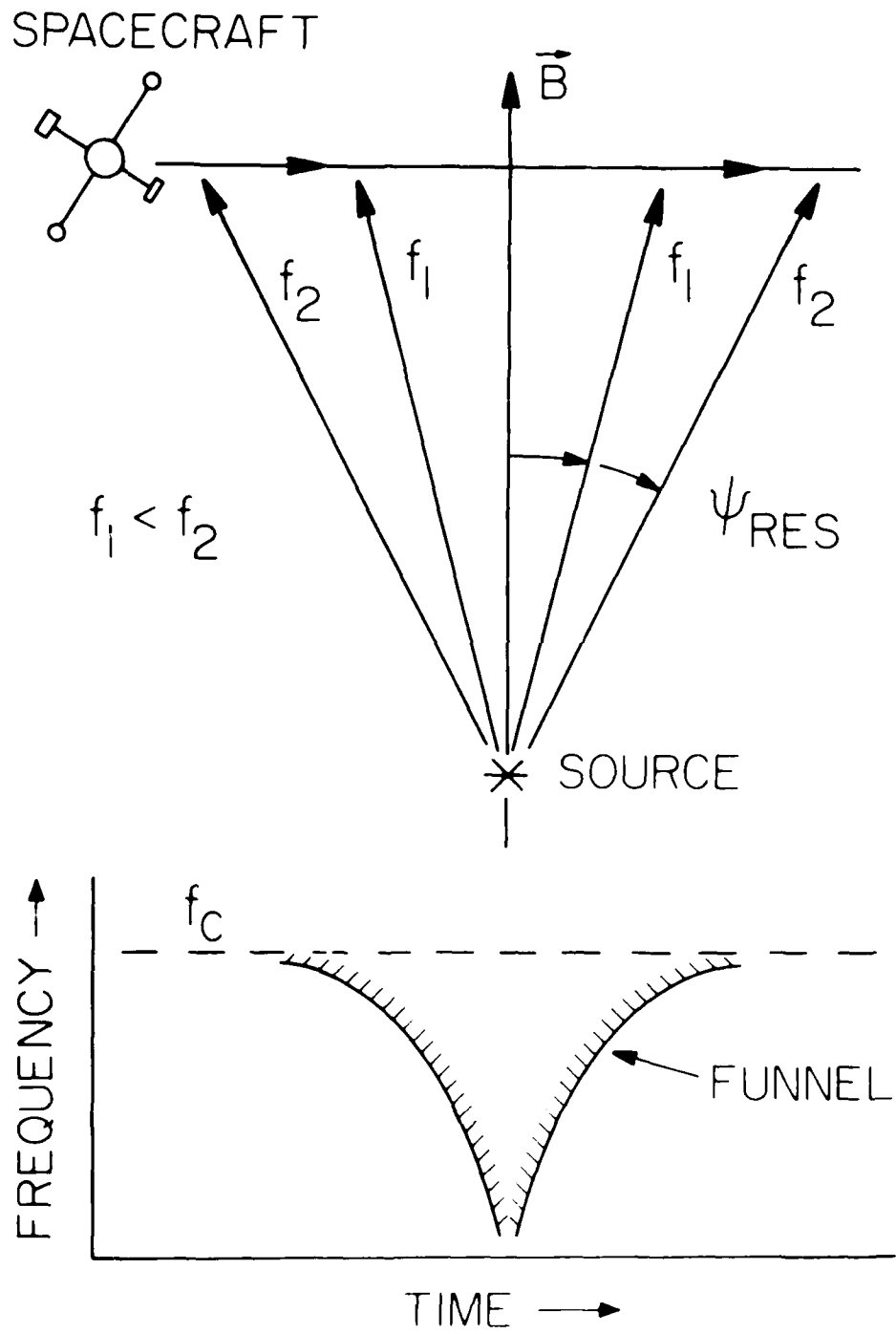


Figure 4

A-G85-855

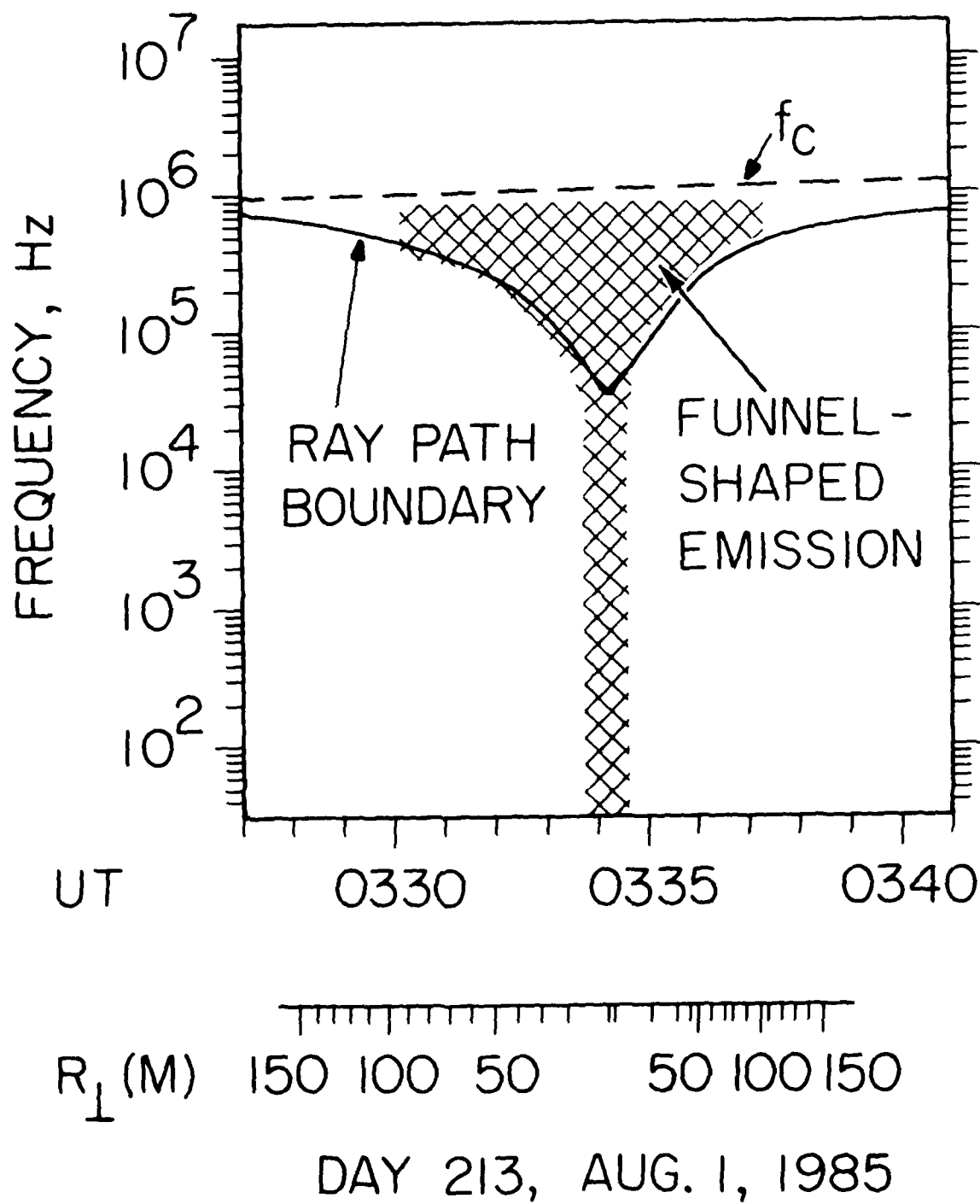


Figure 5

END

FILMED

2-86

DTIC